Geol. Soc. Malaysia, Bulletin 22, December 1988; pp.23–43

Significance of Stylolite Development in Hydrocarbon Reservoirs with an Emphasis on the Lower Cretaceous of the Middle East

RICHARD B. KOEPNICK
Mobil Research and Development Corporation
Dallas Research Division
P.O. Box 819047
Dallas, Texas 75381
U.S.A.

Abstract: Growth of stylolites and related pressure-solution features may adversely affect the continuity of carbonate reservoirs by producing barriers or impedences to fluid flow. The impact of stylolite development on reservoir performance, however, may vary greatly from one part of a reservoir to another. Therefore, it is important to know the distribution and the permeability of stylolites for development of an effective program of reservoir management.

The variable impact of stylolite development is illustrated through analysis of a reservoir case history. In this example, stylolite frequency and cumulative stylolite amplitude increase from the crest to the flanks of the anticlinal closure which constitutes the field. These trends are largely controlled by: 1) the pattern of stress concentration developed during growth of the anticlinal structure and by 2) the inhibition of pressure solution by hydrocarbons along the anticlinal crest. Although stylolites occur throughout the reservoir, three principal zones of stylolite development are of concern with regard to reservoir management. Of the three, only the uppermost zone (D1) is a significant barrier to fluid flow. Variation in permeability among the main stylolite zones probably is related to the timing of stylolite formation with respect to hydrocarbon entrapment. The impermeable stylolite zone (D1) formed largely before hydrocabon entrapment. In this case, abundant crystal nucleation sites are present immediately adjacent to the pressure-solution feature allowing local precipitation of calcium carbonate derived from dissolution along the pressure-solution surface. The remaining stylolite zones (D2 and D3) largely developed during or after hydrocarbon entrapment. Hydrocarbons inhibit precipitation of calcium carbonate by coating many favorable nucleation sites within the reservoir. Thus, the bulk of the calcium carbonate dissolved at pressure-solution surfaces can be transported away from the stylolite zone prior to precipitation. Localized cementation and permeability reduction, therefore, will not occur adjacent to the stylolite zone. Consequently, stylolites developed largely after hydrocarbon entrapment, in this example, do not constitute significant barriers to vertical fluid flow.

INTRODUCTION

The growth of stylolites and related-pressure solution features may adversely affect reservoir continuity by producing barriers or impedences to fluid flow (Dunnington, 1967; Mossop, 1972; Wong and Oldershaw, 1981; Muin and Hastowidodo, 1982). The impact of stylolite development on reservoir performance, however, may vary greatly from one part of a reservoir to another (Figure 1). It is important, therefore, to know both the distribution and the permeability of stylolites or stylolitic horizons. This report summarizes a geologic analysis of stylolites within a Lower Cretaceous carbonate reservoir in the Middle East. The objective is to illustrate the variable impact of stylolite development through analysis of a specific case history.

Presented at CCOP-ASCOPE-GEOSEA WORKSHOP 'Carbonate Diagnesis', 4 – 6 April 1984, Kuala Lumpur

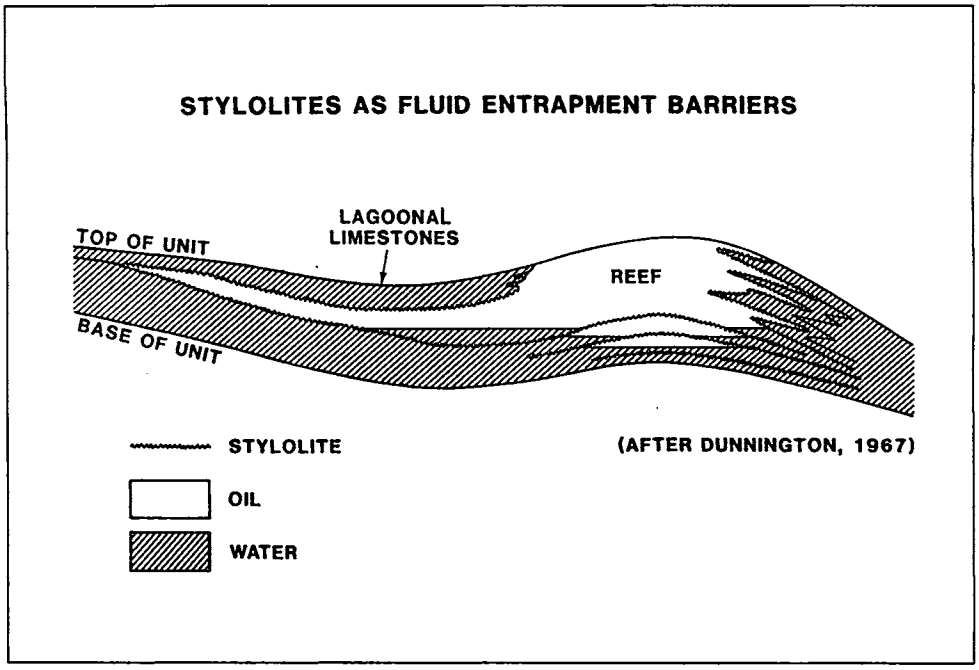

Figure 1: Stylolites as fluid entrapment barriers. Diagramatic cross section cut parallel to axes of folded limestone reef reservoir. At left, stylolites cut oblique to bedding to form a porosity pinch out which limits the extent of reservoir. Beneath the main reef buildup, stylolites compartmentalize the reservoir into producing subunits with different oil/water contacts. At right, stylolites develop parallel to dipping tongues of reef debris. Associated cementation limits water drive capacity and complicates peripheral water injection patterns.

In this example, data from 30 cored wells are presented in contour map form illustrating both field-wide distribution of stylolites within the reservoir, and thickness of cemented intervals associated with major stylolite horizons (Figures 6-9). In addition, the permeability and pore geometry of stylolite-bearing core are evaluated in a series of engineering and geologic tests. Not all stylolites in this field constitute barriers to fluid flow. To illustrate this variability, porosity, permeability, and pore geometry data are presented for two stylolite zones (Figures 11, 12).

ORIGIN OF PERMEABILITY REDUCTION IN THE VICINITY OF PRESSURE-SOLUTION FEATURES

Permeability reduction results from the activity of two distinct processes: 1) pressure solution and 2) solution transfer (Durney, 1976, p. 231). Pressure solution is the process whereby minerals dissolve along grain contacts or along more extensive surfaces, such as stylolites, under the influence of pressure or stress. In a buried sedimentary sequence, pressure at points of grain contact may exceed the average lithostatic pressure. Adjacent free portions of grain boundaries, however, are subjected only to the pressure of the pore fluid which generally is less than lithostatic pressure. Because mineral solubility increases with

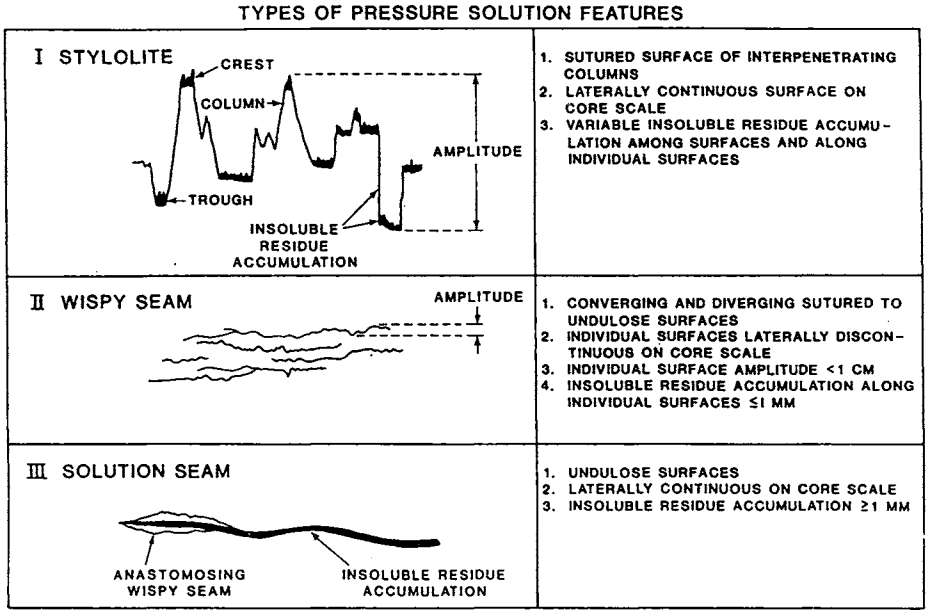

Figure 2: Pressure solution features within the reservoir.

pressure, a decreasing concentration gradient between high-pressure grain contact areas and adjacent low-pressure areas is built up. In response to this gradient, outward diffusion of solute takes place and dissolution occurs either along the sedimentary grain contact zone, or, in the case of stylolites, along the solution surface. Because each sedimentary particle has a slightly different solubility, considerable relief may develop along stylolite surfaces. The relief or amplitude (Figure 2) is generally considered to be a measure of the minimum thickness of sedimentary section removed along the solution surface (Stockdale, 1922, 1926; but also see Sellier, 1983). As pressure solution proceeds, insoluble constituents gradually accumulate along the solution surface (Figure 2). If a continuous film of insoluble residue develops, then significant permeability reduction will occur.

Further permeability reduction may result from matrix cementation adjacent to pressure-solution surfaces. Matrix cementation is a result of the solution transfer process which includes solute transport, and precipitation of minerals derived from pressure-solution surfaces. Transport is controlled by solute diffusion, which is a consequence of the development of a concentration gradient between high pressure contacts along solution surfaces and adjacent low pressure areas. Because diffusion is a slow process, in many cases transport involves movement of both solute and solvent by fluid flow (Bathurst, 1971). Rate of fluid flow very likely affects the distance dissolved constituents are transported prior to precipitation. Transport distance also is affected by the geometry of the concentration gradient, which in turn reflects the overall pressure gradient associated with the pressure-solution surface. Although transport of solute to low pressure areas produces supersaturation,

precipitation may not occur spontaneously. Precipitation depends on the location of favorable nucleation sites for crystal growth. In some cases, abundant nucleation sites may occur immediately adjacent to the solution surface thus riggering local precipitation. In other cases, nucleation sites may be widely scattered with respect to the solution surface, causing widely dispersed cementation. When matrix cementation occurs immediately adjacent to the pressure-solution surface, extensive permeability reduction may result (Figure 11). On the other hand, if dissolved materials are transported beyond the immediate vicinity of the pressure-solution surface, then adjacent matrix permeability remains (Figure 12). As a consequence, the amplitude of pressure-solution surfaces may not show a positive correlation with degree of matrix cementation. In other words, high amplitude stylolites may be weakly cemented whereas low amplitude stylolites may be strongly cemented.

The overall matrix permeability characteristics of pressure-solution features are largely a function of thickness and continuity of insoluble residue and the extent of matrix cementation adjacent to the solution surface. On a field-wide basis, the permeability characteristics of these features also will depend on their lateral continuity and on the abundance of natural fractures cross-cutting their associated zone of matrix permeability reduction.

SUBDIVISION OF PRESSURE-SOLUTION FEATURES

Pressure-solution features can be subdivided informally into three groups: stylolites, wispy seams, and solution seams (Figure 2). The subdivision is based on the amplitude and morphology of the pressure-solution surface, the lateral continuity on core scale of the pressure-solution surface, and the thickness of accumulated insoluble residue along the pressure-solution surface.

Stylolites

Stylolites as described by Park and Schot (1968, p. 175) are:

"recognised as irregular planes of discontinuity between rock units; the irregularities display the shape of "*stylas*", the Greek word for columns and pyramids. Consequently, the two rock units appear to be interlocked or mutually interpenetrating along a very uneven surface. This surface is referred to as a stylolite, which is most commonly characterized by the concentration of relatively insoluble constituents of the enclosing rock."

In this study only stylolites with an amplitude greater than 1 cm are individually recorded and compiled on the contour maps of stylolite distribution and of cumulative stylolite amplitude (Figures 6, 7). Features with smaller amplitudes are difficult to evaluate in terms of amount of section removed, particularly in view of their tendency to form bifurcating and anastomosing swarms (Mossop, 1972, p. 246). Measurement of stylolite amplitude (Figure 2) generally provides a minimum estimate of section removal. This is considered to be a minimum estimate because an unknown amount of dissolution may have occurred on both crest and trough thereby yielding an amplitude that is smaller than the actual amount of section removed. For some types of stylolites, however, the amplitude method may overestimate the amount of section removal (e.g. the rectangular stylolites of Sellier, 1983). Overall, the summation of individual stylolite amplitudes probably estimates the minimum amount

of thinning of section caused by pressure-solution (Figure 7).

For each stylolite, the amplitude and thickness of insoluble residue on both crest and column margin was recorded (Figure 2). The multiple insoluble residue measurements document the lateral continuity on core scale of insoluble residue along individual stylolite seams. Stylolites with thick, laterally continuous insoluble residues constitute more effective barriers to fluid cross flow than stylolites either with thin, laterally continuous insoluble residues or with discontinuous insoluble residues.

Wispy Seams

Wispy seams (Figure 2) are low amplitude, undulose to finely sutured, laterally discontinuous pressure-solution surfaces with insoluble residue thickness of 1 mm or less. Wispy seams are similar to "horsetail stylolites" described by Mossop (1973, p. 246) and to "simple seams" described by Garrison and Kennedy (1977, p. 113). Wispy seams occur individually or in thick, vertically extensive swarms. In spite of the lateral discontinuity of individual seams, swarms of wispy seams may form significant barriers to fluid cross flow and are commonly associated with impermeable stratigraphic intervals in this reservoir example. Permeability reduction is due to development of networks of insoluble residues and to cementation of adjacent pore space through the short-range activity of the solution-transfer process.

Solution Seams

Solution seams (Stockdale, 1922, p. 52) are low amplitude, undulose surfaces with thick accumulations of insoluble residue (Figure 4). These features are similar to "composite seams" described by Garrison and Kennedy (1977, p. 113). Solution seams are laterally continuous on core scale and are often associated with networks of wispy seams and small stylolites. The lateral continuity and thick buildup of insoluble residue make solution seams important barriers to fluid cross flow. Solution seams commonly are associated with impermeable stratigraphic intervals, in this example.

DISTRIBUTION OF STYLOLITES WITH RESPECT TO RESERVOIR LITHOLOGY

The reservoir section is composed of a stratigraphic succession of six compositionally homogeneous, laterally continuous, non-argillaceous limestone units (Figure 3). The reservoir section is overlain and underlain by intervals of dense limestone characterized by abundant pressure-solution features. The reservoir boundaries are marked by changes in intensity of pressure solution rather than changes in character of the depositional environment. Although stylolites occur in all reservoir units, there are three principal zones of stylolite development, identified as D1, D2 and D3, that are of particular concern with regard to vertical fluid flow in the reservoir. These stylolite zones, moreover, are used to define reservoir engineering subzone boundaries (Figure 3). Within the reservoir interval, stylolite development generally is more extensive on the flanks of the structure (Figure 4) than on the crest (Figure 5).

LM Facies

The lime mudstone facies (LM), occurring at the base of the reservoir, is composed of lime mudstone and foram wackestone with extensive leached matrix porosity and minor

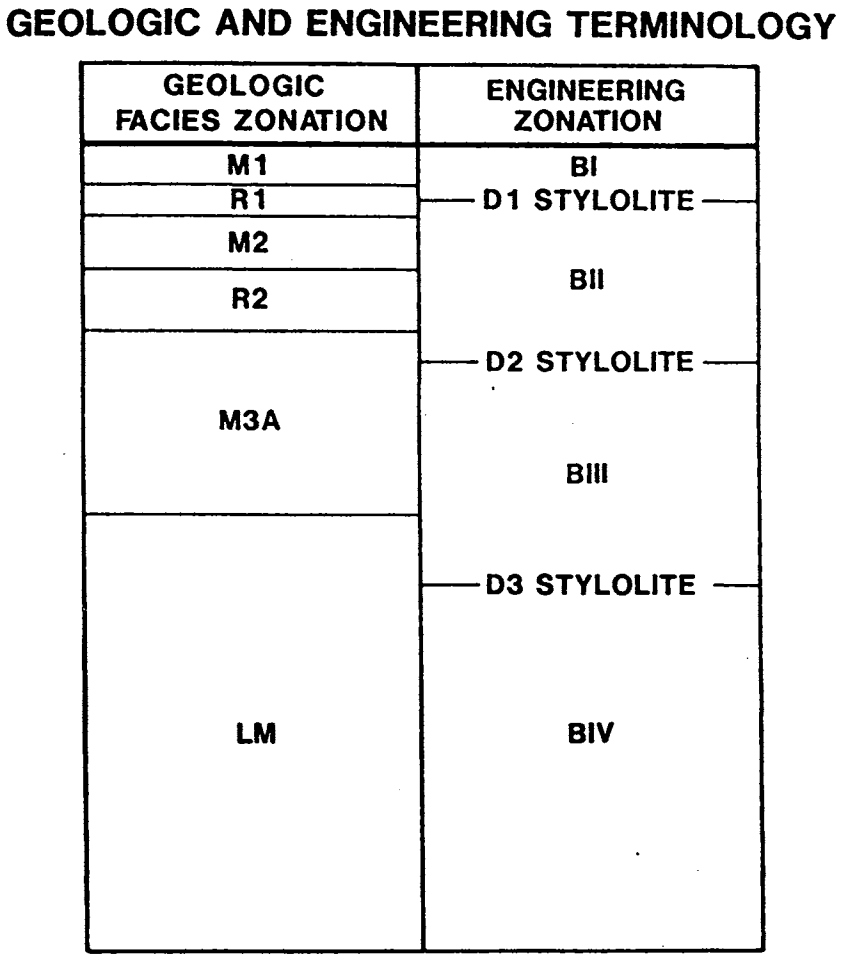

Figure 3: Geologic and engineering reservoir terminology. Figure shows relationship between geologic facies zonation and reservoir engineering zonation (BI, BII, BIII). Note that the D1, D2, and D3 stylolite zones define engineering unit boundaries. By contrast, the styloites do not correspond with geologic facies boundaries.

moldic porosity. The rock types often exhibit scattered dolomite rhombohedra and local patches of dolomite associated with burrows. Dolomite content seldom exceeds 10 percent.

Stylolites within LM generally are hydrocarbon saturated, possess both high surface amplitudes and thin discontinuous insoluble residues, and exhibit minimal associated matrix cementation. The D3 stylolite zone occurs near the top of the LM facies (Figure 3). It commonly consists of 1 or 2 discrete stylolites and rarely exhibits associated wispy seams or solution seams. Additional large stylolites often occur within 10 to 20 feet (3-6 m) of the D3

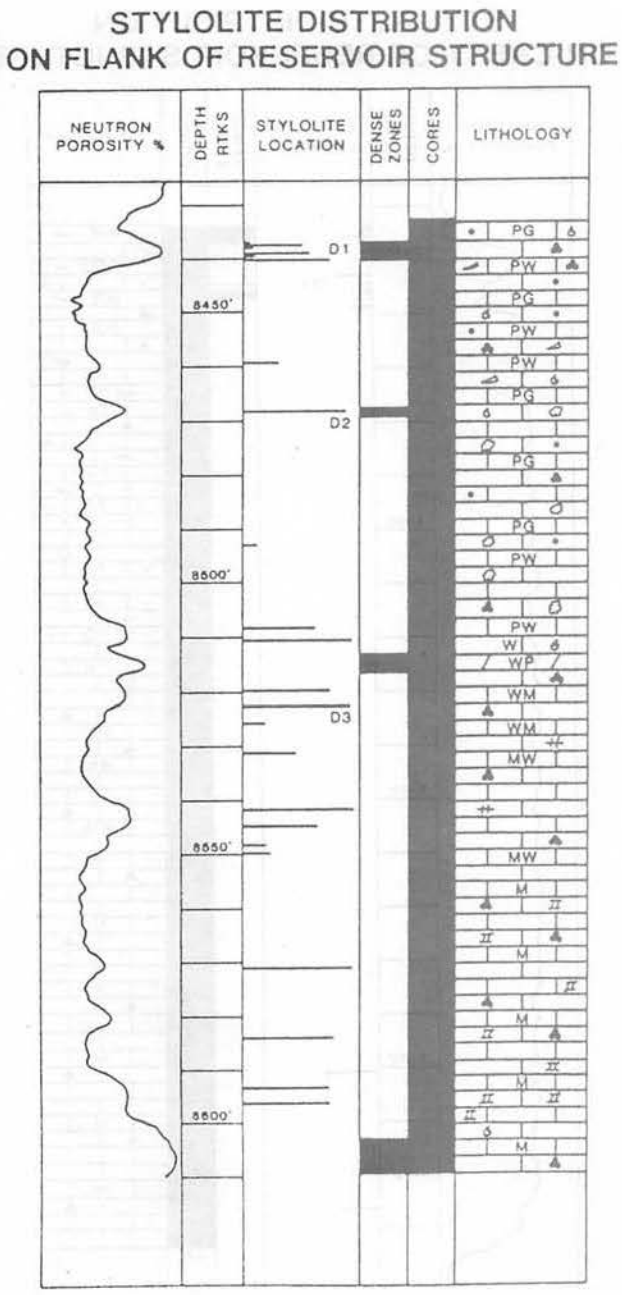

Figure 4: Representative stylolite and lithology log from the flank of the reservoir structure. Note the abundance of stylolites, the presence of the D2 and D3 stylolite zones, and the characteristic log response.

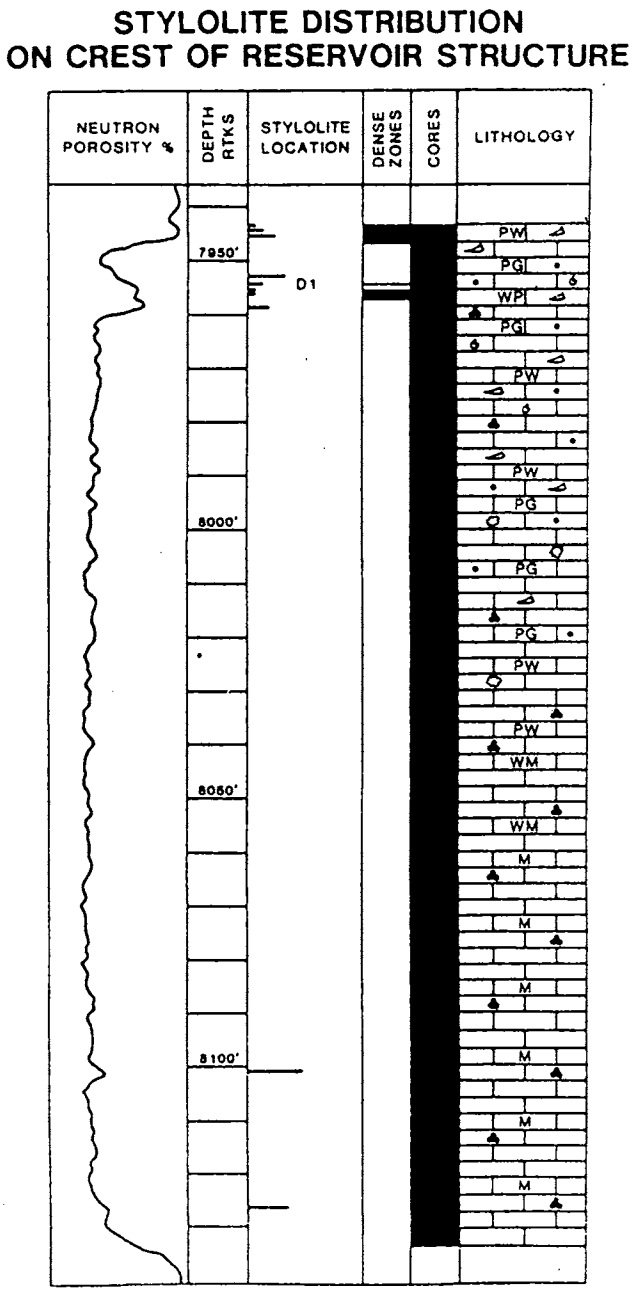

Figure 5: Representative stylolite and lithology log from the crest of the reservoir structure. Note the paucity of stylolites, the absence of the D2 and D3 stylolite zones, and the uniformity of the neutron porosity log.

stylolite as do local zones of extensional fractures and breccia. The D3 locally is absent on the crest (Figure 5) of the structure.

M3A Facies

The miliolid, algal-lump facies (M3A) immediately overlies the LM mudstones and wackestones. In many wells, M3A exhibits an upward lithologic transition from foram, skeletal wackestones to skeletal, algal-lump packstones and grainstones. M3A rock types exhibit leached matrix, moldic, and leached interparticle porosity. Leached interparticle porosity owes its origin to secondary enlargement of primary interparticle pore space and to selective dissolution of interparticle matrix.

The D2 stylolite zone occurs near the top of M3A (Figure 3). It generally consists of 1 or 2 high amplitude stylolites exhibiting thin insoluble residues. Extensional fractures occasionally develop immediately adjacent to the D2 stylolite surface. Visible cementation occurs adjacent to the D2 stylolite over some parts of the field, particularly on the flanks of the reservoir structure, but for the most part it is hydrocarbon saturated and weakly cemented. Locally the D2 stylolite is absent (Figures 5, 9).

R2 Facies

Rudist facies R2 immediately overlies the M3A facies. R2 consists of rudist packstones and wackestones. Rudist density varies geographically and stratigraphically reflecting random stacking of discrete rudist growth centers. R2 exhibits an extremely heterogeneous secondary pore system consisting of leached matrix porosity and large rudist-related molds and vugs. Few stylolites are present in this zone, but numerous wispy seams occur in the matrix between the rudist molds.

M2 Facies

The overlying facies unit, M2, consists of miliolid, pellet grainstones and packstones with numerous micritized composite grains and scattered skeletal debris. M2 grainstones occasionally exhibit cross-bedding and local non-depositional, subaqueous hardground surfaces. M2 rocks exhibit secondary interparticle, moldic and leached matrix porosity. Few stylolites are present within this unit.

R1 and M1 Facies

M2 is overlain by rudist facies R1 which is compositionally identical with rudist facies R2. R1 is much less porous and permeable than R2, however, due to extensive cementation associated with the D1 stylolite zone. R1 lithologies exhibit minor leached interparticle, moldic and leached matrix porosity. Pore space largely is occluded by calcite and dolomite cement and by authigenic kaolinite.

The D1 zone is a complex of stylolites, wispy seams and solution seams producing a 1 to 5 feet (0.3-1.5 m) cemented interval across the reservoir (Figures 8, 11). The D1 interval generally occurs within the R1 facies, but in some cases, the D1 interval overlaps the R1/M1 boundary or occurs entirely in the overlying M1 zone. The M1 miliolid facies is essentially identical to M2 in terms of lithologic composition and pore space development.

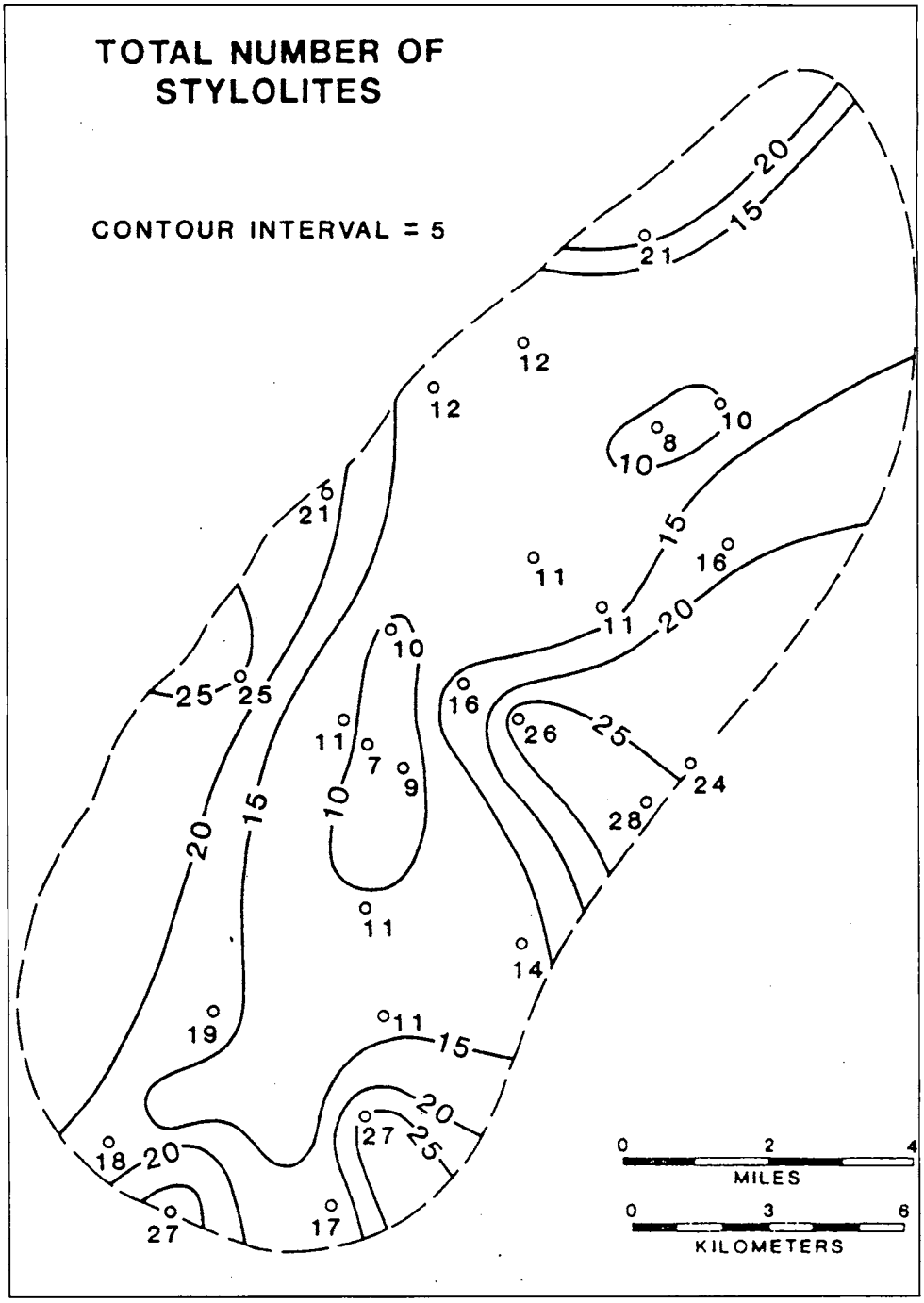

Figure 6: Contour map of total number of stylolites within the reservoir. Map displays field outline, well location and number of stylolites recorded for each well.

FIELD-WIDE DISTRIBUTION OF STYLOLITES

Stylolite data are presented in contour map form to document the field-wide variation in total number of stylolites, and of cumulative stylolite amplitude (Figures 6, 7). The figures show two superimposed patterns: an axial trend developed parallel to the long axis of anticlinal closure which constitutes the field, and a cross-axial trend developed perpendicular to the long axis of the anticlinal closure. The axial trend consists of increasing numbers of stylolites and increasing values of cumulative stylolite amplitude from the crest to the flanks of the structure (also see Figures 4, 5). The cross-axial trend consists of a series of crestward contour deflections representing regions of higher than average numbers of stylolites or larger than average values of cumulative stylolite amplitude. Cross-axial trends produce an irregular, fluted contour pattern around the margins of the field. The maps also show preferential development of pressure-solution features at the southern nose of the anticline.

The contour maps show a systematic distribution of pressure-solution features with respect to the anticlinal structure. A similar pattern is recognized at Bab field, Abu Dhabi (Dunnington, 1967), where stylolite frequency and stylolite-related reservoir thinning increase from the crest to the flanks of the structure (Figure 10). In this case history and at Bab field, stylolite distribution probably reflects a combination of stress concentration patterns developed during growth of the reservoir structures, and of pressure-solution inhibition by hydrocarbon entrapment (Dunnington, 1967). Cross-axial trends and preferential development of pressure-solution features on the southern nose of the anticline in this case history, mainly reflect patterns of local stress concentration developed during structural growth.

CEMENTATION ASSOCIATED WITH D1, D2, AND D3 STYLOLITE ZONES

Figures 8 and 9 document the disribution of visually estimated thickness of cemented rock associated with the D1 and D2 stylolite zones. The D1 contour map (Figure 7) displays strongly developed cross-axial trends of thick and thin D1-associated cementation. The D1 zone is present across the entire field and is not hydrocarbon saturated. The D2 contour map (Figure 9) exhibits a similar but less distinct pattern of cross-axial trends. The D2 interval differs from the D1 interval in that the D2 stylolite is locally absent and that the D2 interval lacks visible cementation over large areas of the field. For the most part, the D3 stylolite interval is not visibly cemented, and, like the D2 interval, is locally absent across the field. Both the D2 and D3 horizons are hydrocarbon saturated. Laterally discontinuous stylolites also are characteristic of Bab field where many horizons die out across the anticlinal crest of the field (Figure 10).

These data suggest that the D1 stylolite horizon constitutes a significant barrier to vertical fluid cross flow by virtue of its lateral continuity and its associated zone of matrix cementation. On the other hand, the D2 and D3 stylolite horizons appear to be less significant barriers to vertical fluid flow by virtue of their lateral discontinuity, weak cementation, and hydrocarbon saturation. These qualitative observations and conclusions are supported in the following section by permeability measurements of stylolite-bearing cores from the D1 and D2 stylolite horizons.

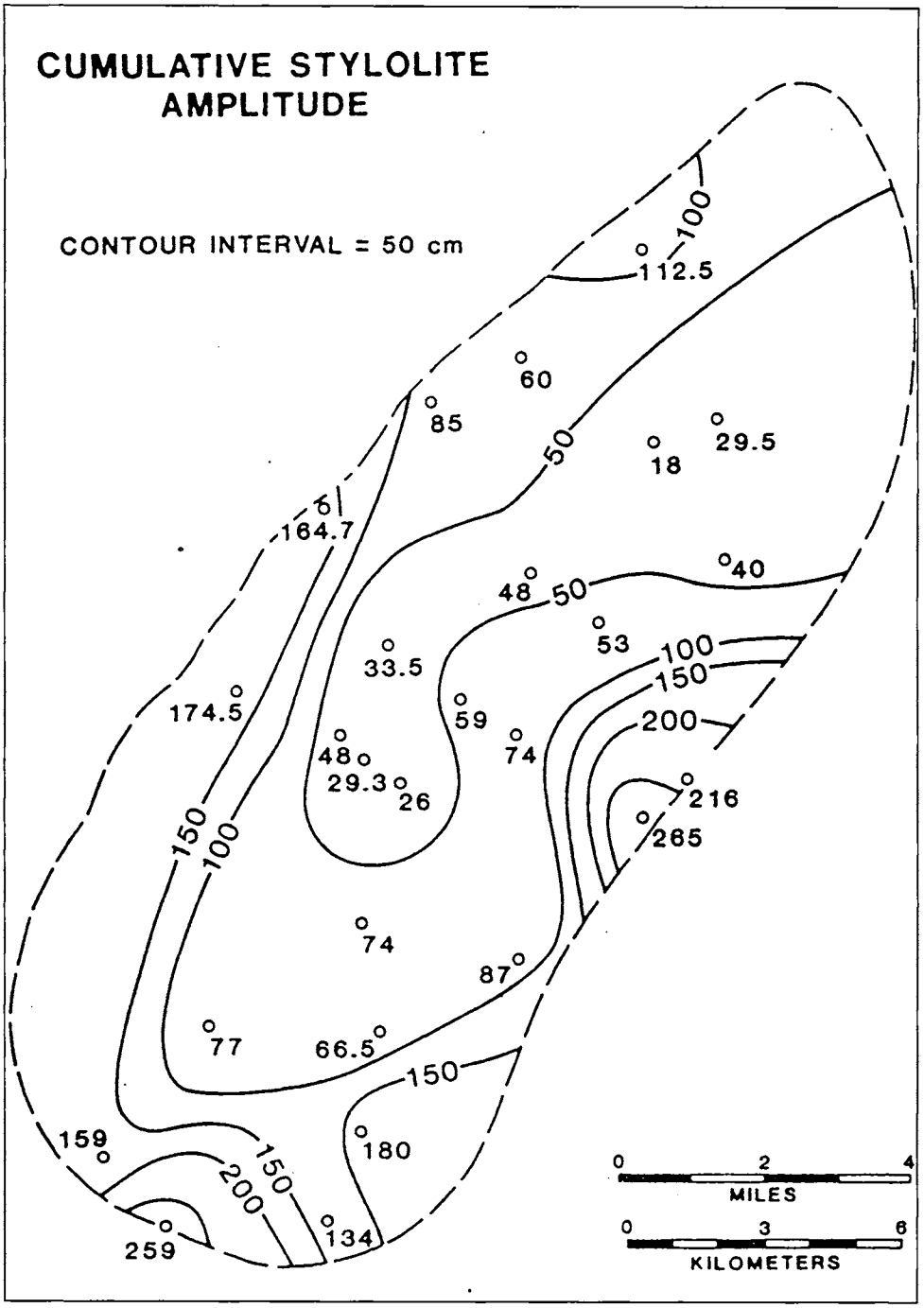

Figure 7: Contour map of cumulative stylolite amplitude for the entire reservoir. Map displays field outline, well location and cumulative amplitude value in centimeters for each well.

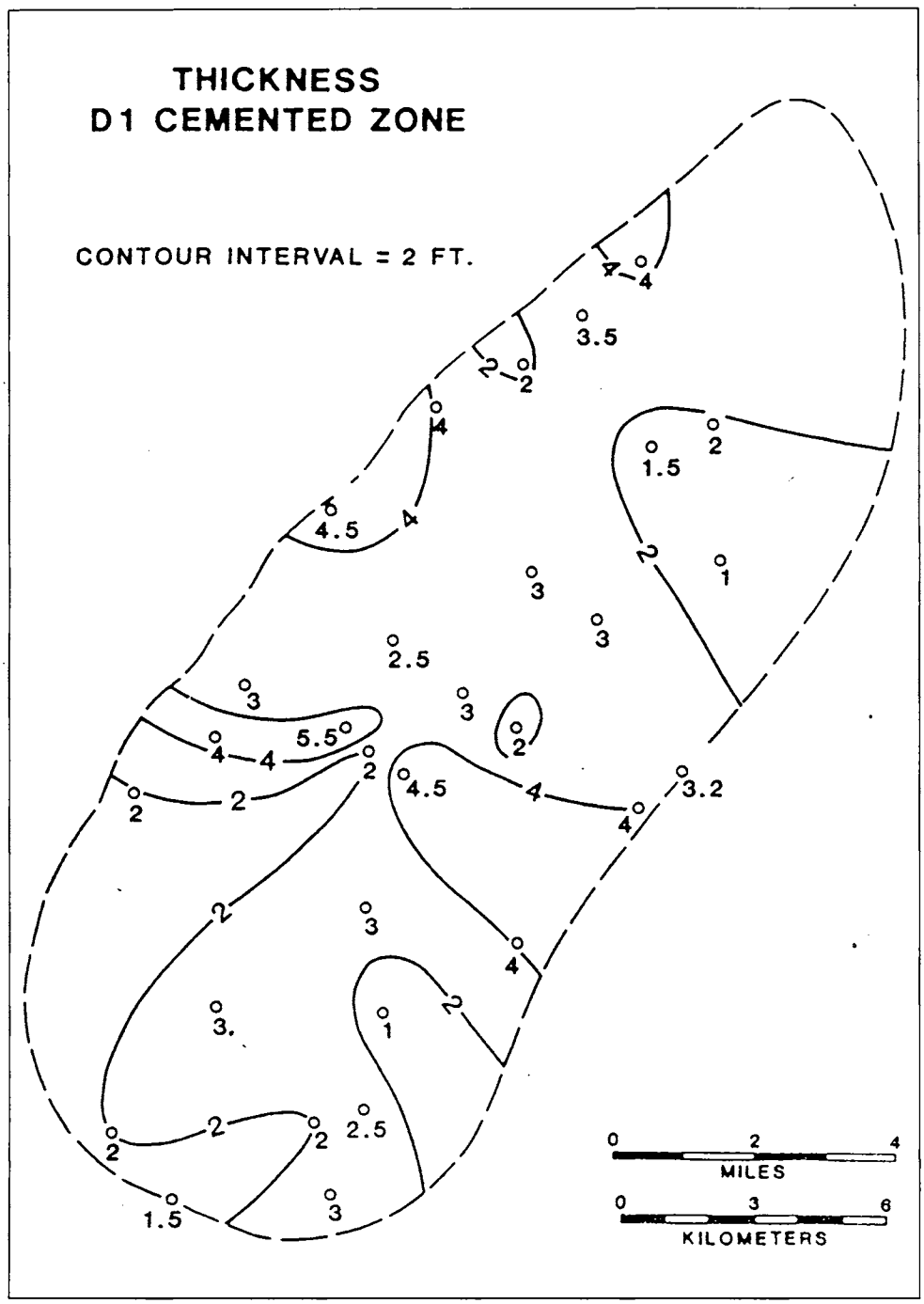

Figure 8: Contour map of thickness of D1 cemented zone. Map displays field outline, well location and thickness values in feet of D1 cemented zone for each well

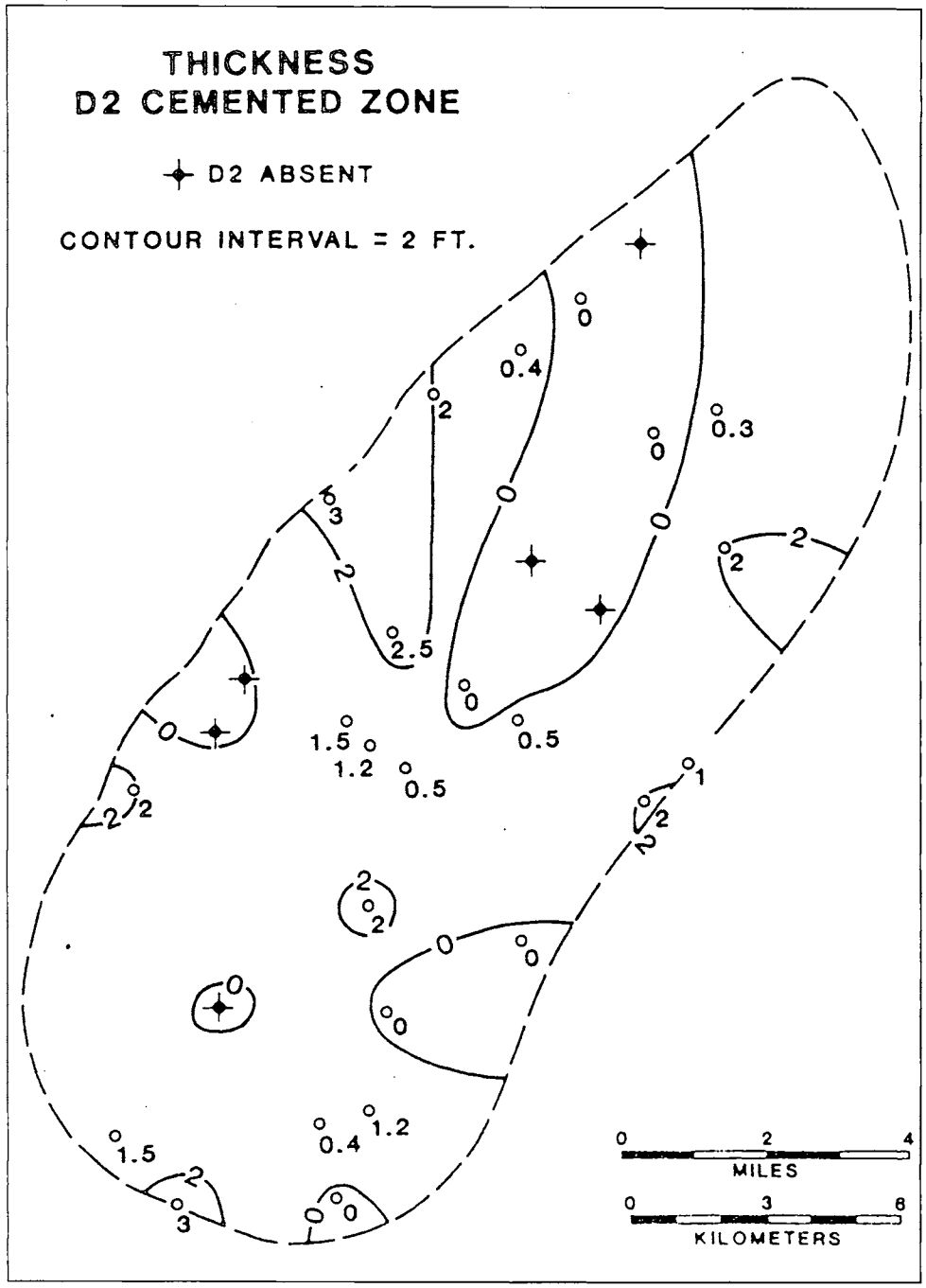

Figure 9: Contour map of thickness of D2 cemented zone. Map displays field outline, well location and thickness value in feet of D2 cemented zone for each well

CHANGES IN VERTICAL PERMEABILITY AND PORE GEOMETRY OF CORE MATERIAL IN THE VICINITY OF THE D1 AND D2 STYLOLITE ZONES

The major stylolite zones D1, D2, and D3 constitute potential barriers to fluid cross flow in this reservoir. To illustrate the variability of permeability reduction associated with these features, measurement of vertical permeability to air was completed on full diameter, stylolite-bearing core and on vertical plugs cut at spaced intervals across a D1 and D2 stylolite zone. The full diameter and plug data are presented in a stratigraphic context, together with a detailed stylolite and lithology log (e.g. Figure 11). In addition to porosity and permeability, the following measurements and analyses are presented for each plug: 1) pore entry radius and pore entry radius distribution by mercury injection and 2) surface area measurement of plug pore space by nuclear magnetic resonance (NMR). The porosity, permeability, mercury injection, and nuclear magnetic resonance data are presented for a D1 and a D2 stylolite zone (Figures 11, 12).

D1 Stylolite Zone

The D1 stylolite zone (Figure 11) exhibits a systematic downward decrease in porosity and permeability. This trend corresponds with a systematic change from hydrocarbon-saturated, porous rocks at the top of the interval to unsaturated, cemented rocks at the base of the section.

Both median pore entry radius and pore entry radius distribution display patterns of decreasing values that are similar to the patterns for porosity and permeability (Figure 11). Wide pore entry radius distribution typifies most of the section. The extremely wide pore entry radius distribution at 8028'8" reflects particularly heterogeneous pore space development within a composite-grain grainstone interval.

The NMR surface area data do not correlate well with the porosity and permeability trends. This probably reflects both inherent differences in abundance of microporosity among the various rock types in this section and preferential cementation of larger pores. The surface area contribution of large pores is relatively small so that cementation of the large pores in a sample should have little effect on total NMR surface area. The mercury injection data for pore entry radius distribution show that a wide range of pore entry radii are maintained across the interval in spite of a downward decrease in porosity and permeability. It appears, therefore, that cementation does not significantly alter lithologically controlled variation in microporosity (probably intraparticle porosity) across this interval.

Overall, the D1 stylolite zone exhibits similar geologic and engineering characteristics across the entire field. The visually estimated thicknesses of cemented section in the vicinity of the stylolite seams is about the same (Figure 8) and the permeability reduction across the cemented zone appears to be as strong on the crest as on the flank of the structure. The full core and plug data, together with the lateral continuity of the D1 interval (Figure 8) and lack of hydrocarbon saturation indicates that this feature is an important barrier or impedence to fluid cross flow.

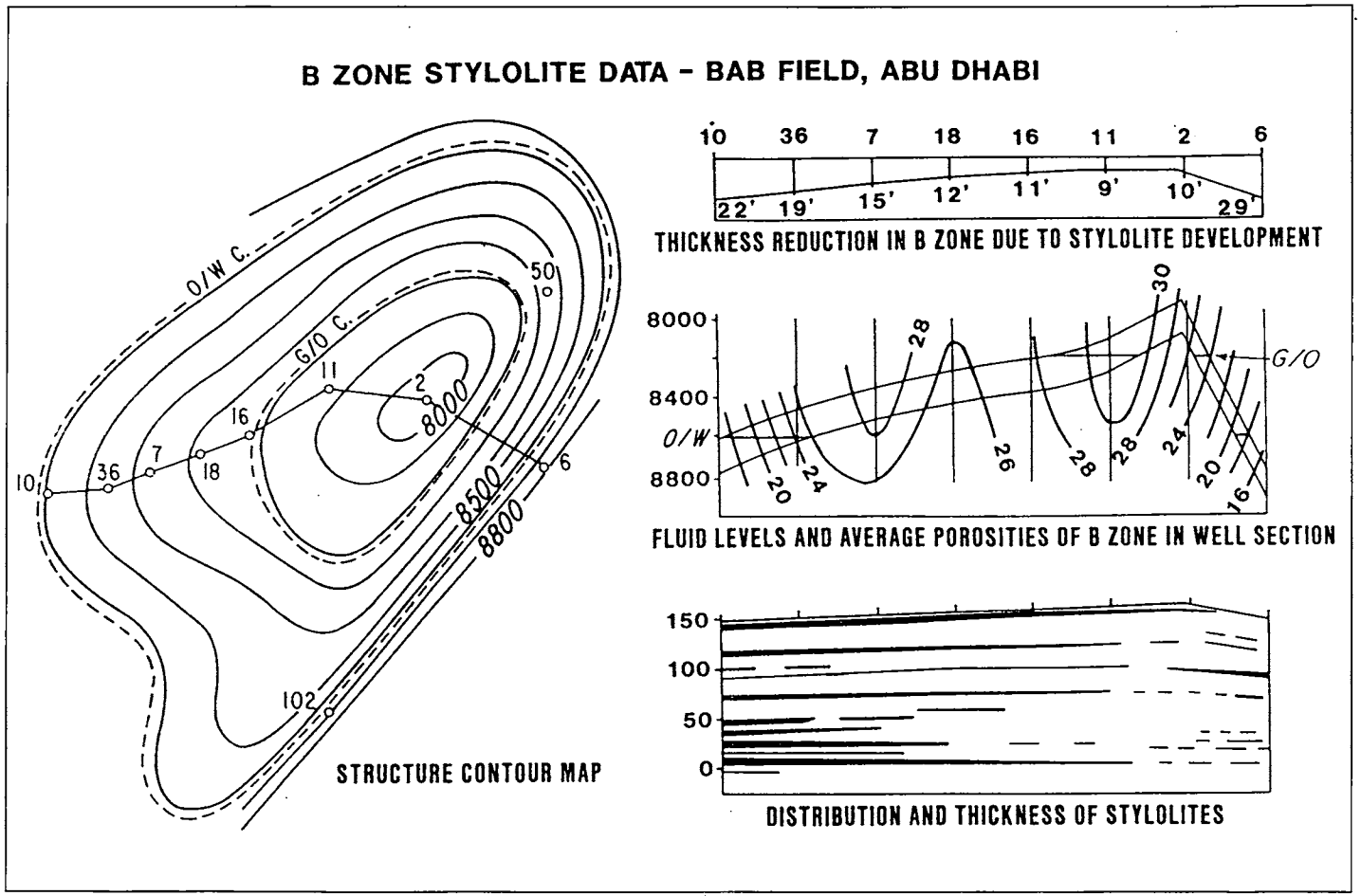

Figure 10: Distribution of stylolite horizons with respect to porosity and to reservoir thickness at Bab field, Abu Dhabi. Both porosity decrease and reservoir thining coincide with increased numbers of stylolites.

D2 Stylolite Zone

The D2 interval exhibits little variation in porosity and permeability across the stylolite zone (Figure 12). The entire section is hydrocarbon saturated.

The interval exhibits extensive leached matrix and leached interparticle porosity, wide pore throat size distributions and high NMR surface area values (Figure 12). Plugs with extremely wide pore entry radius distribution and high NMR surface area between 7937' and 7938' owe their origin to a particularly heterogeneous pore space development within a coarse-grained, algal-lump, composite-grain grainstone/packstone interval.

The D2 stylolite zone exhibits substantial preservation of matrix porosity and permeability. Unlike the D1 zone, however, the D2 locally shows greater cementation and pore geometry alteration along the flanks of the anticline than on the crest (Figure 9). The plug and full diameter permeability data, the lateral discontinuity of the D2 zone, and the extensive hydrocarbon saturation of the D2 zone indicate that this feature is not an important barrier to fluid cross flow in this reservoir.

DISCUSSION

The variation in permeability and diagenetic alteration between the D1 and D2 stylolite zones probably is related to the timing of stylolite growth with respect to hydrocarbon entrapment. The D1 zone is largely devoid of hydrocarbon stain which suggests matrix cementation prior to substantial input of reservoir hydrocarbon. Without hydrocarbons in the pore system, abundant nucleation sites are available nearby for precipitation of solute derived from pressure solution surfaces. Under these circumstances an impermeable horizon should develop immediately adjacent to the pressure solution surface.

The D2 stylolite, on the other hand, is uncemented and is extensively saturated with hydrocarbons. These characteristics suggest that growth of the D2 stylolite zone began during or after hydrocarbon entrapment. Hydrocarbons probably inhibited precipitation of solute derived from pressure-solution surfaces by coating many nucleation sites within the reservoir. This permitted the bulk of the dissolved calcium carbonate to be transported away from the pressure-solution surface prior to precipitaion. Along the anticlinal crest of the structure, growth of the substantially uncemented D2 stylolite probably continued until hydrocarbon saturation increased to the point where it was no longer possible to transport solute through a continuous aqueous medium. Beneath the original oil-water contact, however, inhibition of local solute precipitation probably decreased after the main phase of hydrocarbon migration, and local precipitation of solute derived from pressure solution surfaces probably increased. This may explain why the thickness of cemented limestone in the vicinity of the D2 stylolite generally increases from the crest to the flanks of the structure (Figure 9). Preferential stylolite-related cementaion of the water leg also is documented at Bab field (Figure 10) and at Dukhan field, Qatar (Figure 13). The practical consequences of water leg cementation for reservoir management can include limitation of natural water drive capacity and complication of peripheral water injection patterns.

D1 STYLOLITE INTERVAL

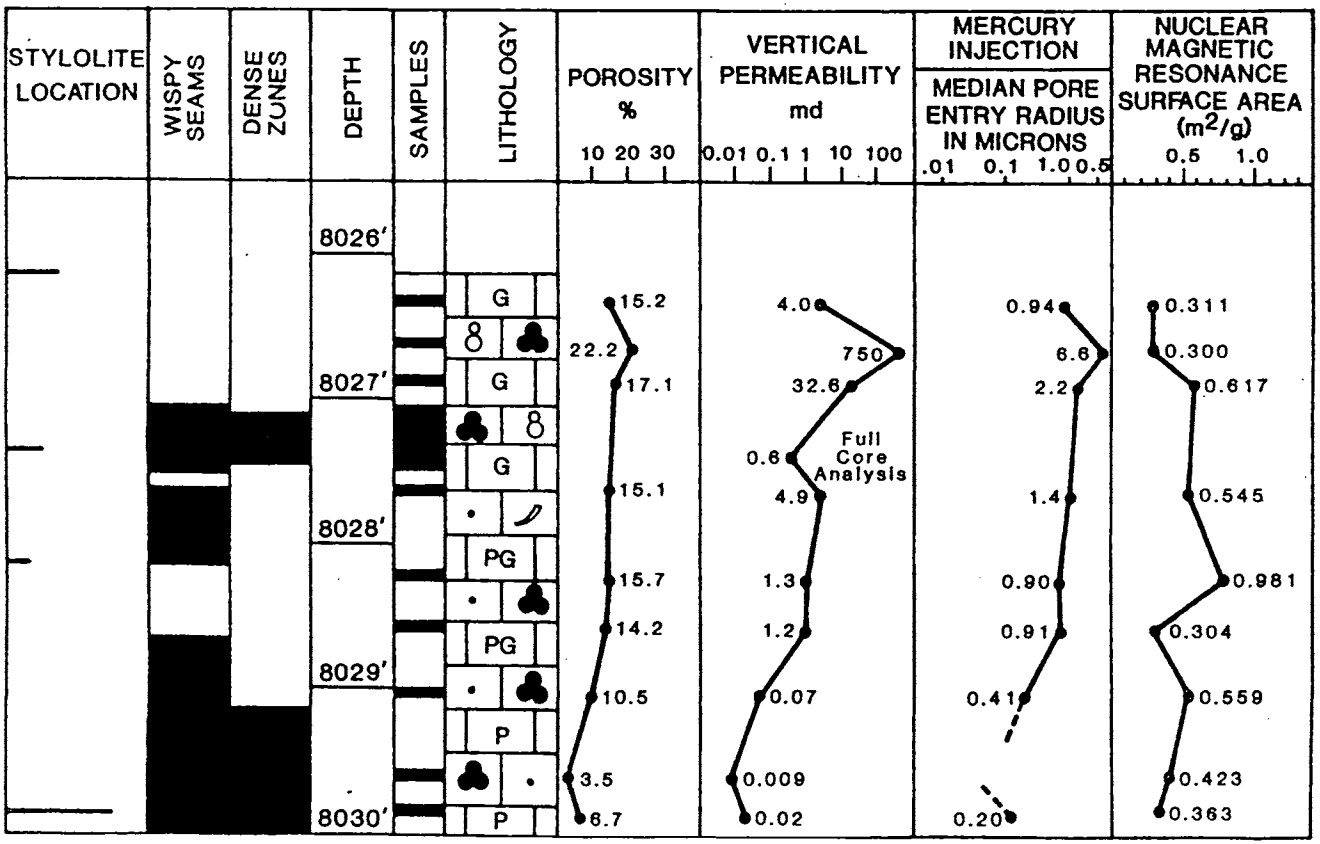

Figure 11: Petrologic and engineering data summary for D1 stylolite interval.

D2 STYLOLITE INTERVAL

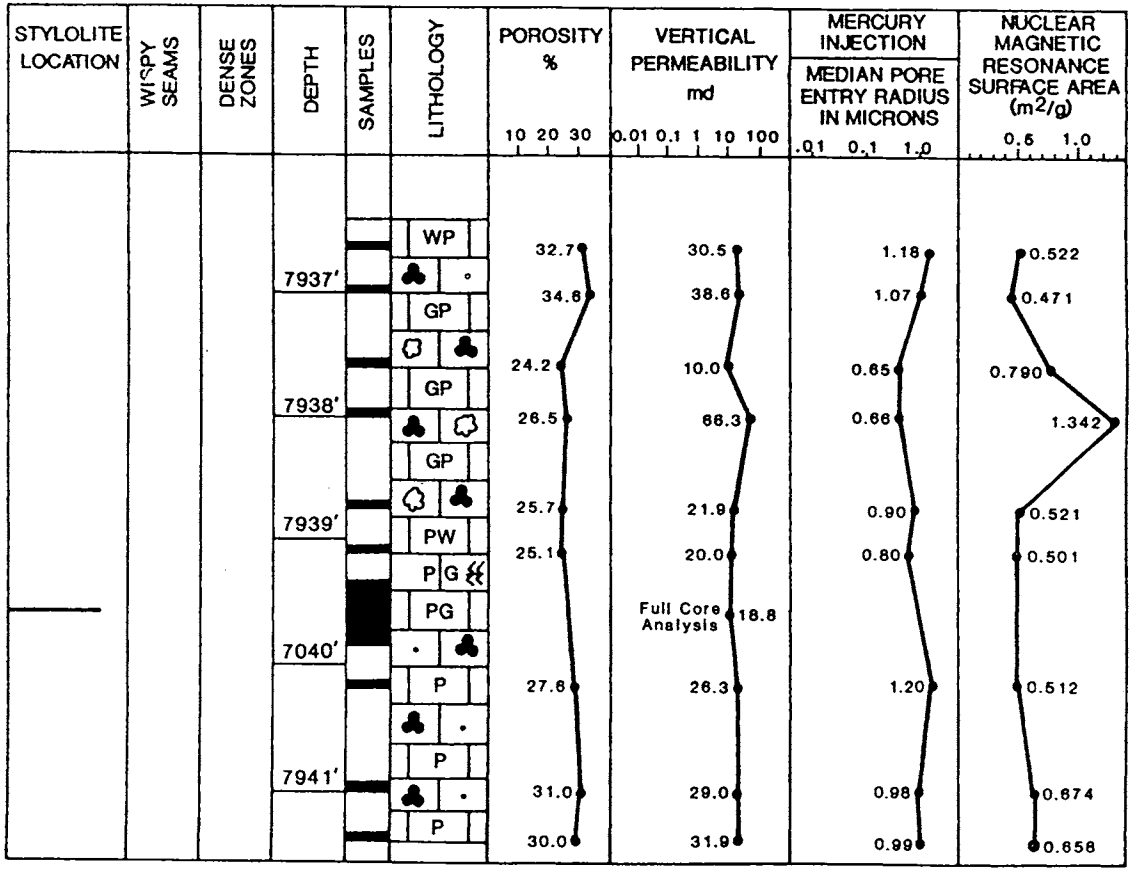

Figure 12: Petrologic and engineering data summary for D2 stylolite interval.

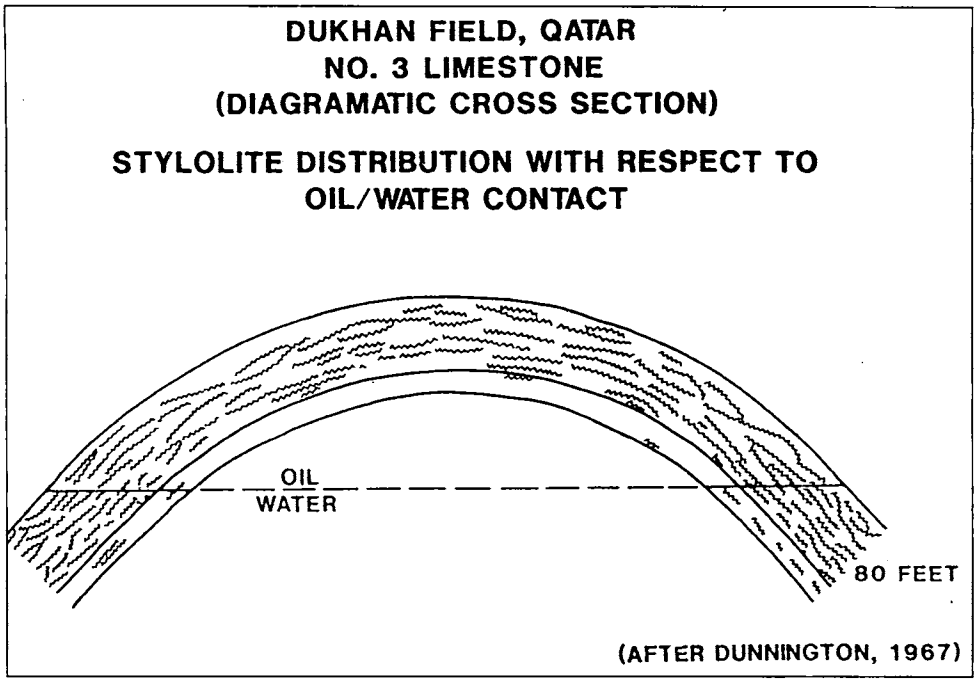

Figure 13: Diagramatic cross-section through No. 3 Limestone, Dukhan field, Qatar, illustrating distribution of stylolites with respect to oil/water contact. Styolite-related cementation below oil/water contact limits drive capacity of aquifer.

CONCLUSIONS

1. The impact stylolites on reservoir performance can vary greatly from horizon to horizon. Consequently, it is important to know the distribution and permeability of stylolitic horizons for development of an effective program of reservoir management.

2. Stylolite distribution in this reservoir is controlled by stress concentrations developed during growth of the anticlinal closure and by differential inhibition of stylolite growth by hydrocarbon saturation.

3. Matrix permeability variation among the D1, D2, and D3 zones probably reflects timing of stylolite growth with respect to hydrocarbon saturation. The D1 stylolite zone largely developed before hydrocarbon entrapment, whereas the D2 and D3 zones largely developed during and after hydrocarbon entrapment.

4. The D1 stylolite is a significant barrier to fluid cross flow and should have a major effect on production characteristics of this reservoir.

5. Both D2 and D3 stylolites are much less important barriers to fluid flow. Both zones are literally discontinuous, weakly cemented, and associated with fractures that partly offset reduction in matrix permeability.

REFERENCES CITED

BATHURST, R.G.C., 1971. *Carbonate sediments and their diagenesis: Developments in Sedimentology 12*, Elsevier, New York 620 p.

DUNNINGTON, H.V., 1967. Aspects of diagenesis and shape change in stylolitic reservoirs: *World Petroleum Congr., Proc., v. 7,* p. 339-352.

DURNEY, D.W., 1976. Pressure-solution and crystallization deformation: *Phil. Trans. R. Söc. London Ser. A,* v. 283, p. 229-240.

MOSSOP, G.D., 1972. Origin of the peripheral rim, Redwater Reef, Alberta: Bull. *Canadian Petroleum Geology,* v. 20, no. 2, p. 238-280.

MUIN, A., and HASTOWIDODO, 1982. Diagenesis and porosity occlusion in stylolitic limestone (an example from Arun Limestone): Joint *ASCOPE/CCOP Workshop on Hydrocarbon Occurrence in Carbonate Formation,* Aug. 2-7, Surabaya, Indonesia.

PARK, W.C., and SCHOT, E.H., 1968. Stylolitization in carbonate rocks. *In*: Muller, G., and Friedman, G.M. (Eds), *Recent Developments in Carbonate Sedimentology in Central Europe*, p. 66-74, Springer, Berlin.

SELLIER, E., 1983. The mechanical approach as an hypothesis for stylolite genesis: *Abu Dhabi National Reservoir Research Foundation El Ain, United Arab Emirates (ADREF) Seminar on Stylolites,* Session 1, No. 3.

STOCKDALE, P.B., 1922. Stylolites: their nature and origin: *Indiana Univ. Studies,* v. 9, p. 1-97.

STOCKDALE, 1926. The stratigraphic significance of solution in rocks: *Jour. Geology,* v. 34, p. 399-414.

WONG, P.K., and OLDERSHAW, A., 1981. Burial cementation in the Devonian, Kaybob Reef Complex, Alberta, Canada: *Jour. Sed. Petrology,* v. 51, no. 2, p. 507-520.

Manuscript received 4 April 1984